Substantial Doppler broadening of atomic-hydrogen lines in DC and capacitively coupled RF plasmas

Kamran Akhtar[1], John E. Scharer[2], and Randell L. Mills[1]
[1] BlackLight Power, Incorporated
493 Old Trenton Road, Cranbury, New Jersey 08512

[2]Department of Electrical and Computer Engineering
University of Wisconsin-Madison, Wisconsin 53706

The mechanism of extraordinary broadening of the Balmer lines of hydrogen admixed with Ar or He as opposed to Xe in a DC glow discharge and a capacitively coupled rf discharge is studied over a wide range of pressure and gas compositions. High-resolution optical emission spectroscopy is performed parallel to the electrode axis (end-on) and perpendicular to the electrode axis (side-on) along with Langmuir probe measurements of plasma density and electron temperature for the capacitive discharge case. An excessively broad and symmetric (Gaussian) Balmer emission line corresponding to 20-60 eV of hydrogen atom energy is observed in Ar/H_2 and He/H_2 plasmas when compared to the majority species atom temperatures. Energy is transferred selectively to hydrogen atoms whereas the atoms of admixed He and Ar gases remain cold (<0.5 eV). In the field acceleration model that has recently been put forth to explain the broadening [Cvetanovic et. al. J. App. Phys., Vol. 97, 033302-1, 2005], there is neither a preferred ion nor atom and according to this model, one should observe enhanced temperature hydrogen and helium atoms in He/H_2 discharges where the atomic mass is more comparable (4:1). The absence of hot H atoms in Xe/H_2 plasmas also challenges the paradigm of the field acceleration model since Xe is also a noble gas and electronically similar to He. The model of an energetic chemical reaction of hydrogen [Mills et. al *IEEE Trans. Plasma Sci.*, 31, p.338, 2003] as the source of broadening can explain the observation that only the selective heating of hydrogen atoms in certain plasmas exhibits the selective extraordinary broadening and isotropic emission profiles.

I. INTRODUCTION

Substantial Doppler broadening of hydrogen Balmer lines has been observed in pure hydrogen and specific gaseous mixtures of hydrogen with certain heavier atom plasmas produced by DC and capacitively coupled 13.56 MHz radio frequency waves [1-17]. This broadening is caused by the presence of excited hydrogen atoms. In all these instances, energy is transferred selectively to the hydrogen atom whereas the H_2 molecules as well as the He and Ar atoms remain cold. Historically, most mechanisms proposed for excessive H_α broadening in pure hydrogen and mixtures of hydrogen with inert gases [1-14] are explained in terms of energetic ions (H^+, H_2^+ and H_3^+) that are accelerated in the cathode fall region followed by energy transfer to the matrix gas (H and H_2) through charge exchange collisions. However, there are variations in the proposed theoretical explanations of the mechanisms that provide energy to atomic H and cause the observed enhanced blue-shifted H_α spectra width that is symmetric with respect to the red-shifted portion of the emission profile. It should be noted, however, that none of these mechanisms explains the selective transfer of energy to the hydrogen atomic state with the atoms of the admixed gases remaining cold (<0.5 eV).

In a pure hydrogen discharge, the Doppler-broadened profile exhibits the presence of a bimodal (or a tri-modal) distribution of neutral species temperatures [14]. The profile consists of a central peak that corresponds to slow thermal hydrogen atoms with kinetic energies in the range 0.25 to 1.0 eV. The population of warm H atoms (10-20 eV) is evident in the plateau of the Doppler broadened profile along with a population of fast hydrogen atoms (> 40 eV). There is general agreement on the mechanisms proposed for the production of slow H (~0.1-1.0 eV) atoms in the excited n=3 state through the process of dissociative excitation, $H_2 + e^- \rightarrow H_2^* + e^- \rightarrow H^*(n=3) + H$, and dissociative ionization,

$H_2 + e^- \rightarrow 2e^- + H_2^+ \rightarrow H^*(n=3) + H^+$, of hydrogen molecules and electron impact excitation of H atoms, $H + e^- \rightarrow e^- + H^*(n=3)$ [1-2].

There are significant variations in the literature describing the mechanisms proposed to explain the production of hydrogen atoms with energies greater than 20 eV. These were originally proposed to be the result of dissociation of H_2^+ ions in vibrationally excited molecular ground states [2-3]. Recently, the mechanism of charge exchange between ions accelerated in the sheath and neutrals and ion impact on electrodes has been proposed as the source of energetic hydrogen atoms in these discharges. In this model, henceforth called the Collisional Model (CM) [5 and references therein], sheath accelerated H^+ and H_3^+ ions in a hydrogen plasma are proposed to either transfer charge directly to the hydrogen atom or dissociate the H_2 molecule followed by charge exchange collisions to explain the energy spectrum of hydrogen atoms [1-15]. The processes are governed by the following reactions [5-7] where the * indicates excited n=3 atomic state:

$$(H^+)_{fast} + H_{slow} \rightarrow H^*_{fast} + (H^+)_{slow} \qquad (1)$$

$$(H^+)_{fast} + (H_2)_{slow} \rightarrow H^*_{fast} + (H_2^+)_{slow} \qquad (2)$$

$$(H_3^+)_{fast} + H_{slow} \rightarrow H_3 + H^*_{fast} + (H_2^+)_{slow} \qquad (3)$$

$$(H_3^+)_{fast} + (H_2)_{slow} \rightarrow H^*_{fast} + (H_2)_{fast} + (H_2^+)_{slow}. \qquad (4)$$

Since the particle acceleration due to the electric field is directional, the energy gained by a positive ion as it travels towards the cathode will maintain that directionality along with the directed energy of the excited hydrogen atom as long as ion-neutral collision rates are small. This mechanism can only account for the red portion of the spectrum when viewed optically towards the ion accelerating electrode sheath. The observed symmetry in the Gaussian profile of the

hydrogen Balmer line is explained in terms of the sputtered fast H atoms and the back-reflected fast H atoms from the cathode surface [5]. It is argued that this will give rise to a symmetric distribution of energetic H atoms leaving the cathode compared to those accelerating towards the cathode.

In the presence of inert gases, the additional process of charge transfer has been proposed to explain the symmetric H_α broadening [3,12-13]. The introduction of Ar in a pure H_2 plasma increases the Balmer line emission intensity that implies that the concentration of excited hydrogen atoms in the excited n=3 state is also increased. In addition, the fractional population of hot hydrogen atoms obtained from the area under the Gaussian curve implies a concentration in excess of 80 percent of the population in the n=3 state. It has been suggested in the above articles that energetic Ar^+ ions dissociate and ionize H_2 to form ArH^+ that enhances the population of H_3^+ that is proposed as the primary source of atomic hydrogen as shown below when Eq. (6) is combined with Eq. (4).

$$Ar^+ + H_2 \rightarrow ArH^+ + H \qquad (5)$$

$$ArH^+ + H_2 \rightarrow H_3^+ + Ar \qquad (6)$$

The role of metastable argon ions in the enhanced production of H_3^+ ions through the formation of molecular hydrogen ions has also been emphasized [6].

$$Ar^+(3p^5\,^2p^0_{1/2}) + H_2 \rightarrow Ar + H_2^+ \qquad (7)$$

$$H_2^+ + H_2^+ \rightarrow H_3^+ + H \qquad (8)$$

It has been suggested in the above articles that the contribution of these pathways to the significant production of H_3^+ in Ar/H_2 results in an enhanced population of energetic H_{fast} atoms through the processes described in Eqns. (3-4).

However, some of the recent observations [17-26] in DC and capacitively coupled rf discharges are in contrast to the field acceleration based Collisional Models described earlier. For example, it is important to note that, to the best of our search of the scientific literature, no experimental observation has ever been reported, including results in this paper where equally energetic atoms of admixed gases have been found even when the plasma is collisional and mass ratios are comparable. The energy is transferred selectively only to the hydrogen atom whereas the electron energy is less than few eV and admixed gas atoms remain cold (<0.5 eV). It is also very intriguing that no hot H atoms are observed when the admixed gas is xenon. In the CM, the energy of the hot H atom should be independent of the nature of the background gases except for differing collision cross-sections with the background gas. Therefore, it is not possible to readily explain the presence of broadening in argon/hydrogen and helium/hydrogen plasmas along with the absence of broadening in xenon/hydrogen plasmas using this model. In addition, the observation of comparably hot hydrogen atoms in regions outside the plasma sheath requires the local creation of energetic H atoms. As discussed later, the rapid thermalization of H atoms with the background gas due to short ion-neutral collision mean free paths should also confine fast H near the region where it is formed. Therefore, only a process where hot H is produced locally can explain the comparable energies of hot H observed well outside the plasma sheath regions.

It should be noted however, that these observations demonstrate that the source of these hot H atoms is a process fully consistent with the Mills' model of energy production known as Resonance Transfer Model (RTM) [17-26]. The RTM predicts excessive broadening due to a novel energetic chemical reaction of H with certain catalysts involving a two-step energy transfer. First, resonant energy transfer occurs from H to a catalyst and then a second radiative emission or a resonant energy transfer to another H atom that serves as a third body to take away

the remaining reaction energy [19-20]. In this model, it is postulated that the electron in the hydrogen atom that undergoes a 'catalytic' reaction that allows decay from the 'conventional' ground state (principal quantum number, n=1) to a 'fractional' quantum state (e.g. n=1/2). Since the ionization energy of hydrogen is 13.6 eV, two hydrogen atoms can also provide a net enthalpy equal to the potential energy of the hydrogen atom, 27.2 eV— the necessary resonance energy, for a third hydrogen atom to form H (n=1/2).

In order to clarify the underlying mechanism of hydrogen Balmer alpha broadening in hydrogen plasmas and plasmas of hydrogen admixed with noble gases and test the validity of field acceleration based Collisional Model (CM) [5], a comprehensive experiment that covers a wide range of gas pressure and plasma parameters has been performed. A DC glow discharge with pin electrodes and a capacitively coupled radio frequency plasma over a wide pressure range (three orders of magnitude – 10 mTorr to 10 Torr) along with different gas mixture ratios are used to test the ability of the CM to explain the unusual nature of the observed hydrogen broadening. As suggested by the CM, the degree of symmetry of the plasma emission profile should be a function of the electron-neutral and ion-neutral collision frequency and, therefore, should depend on the neutral gas pressure. The CM mandates that observations parallel and perpendicular to the electric field lines yield different emission profiles if the collisional scattering rate is sufficiently small. The experimental setup allows observations both parallel and perpendicular to the electrode axes to test this property. In addition, the presence of hot H atoms was examined in regions far away from the high electric field plasma sheath region near the electrodes. The CM also implies that the energy of hot H atoms is independent of the nature of admixed gases. In contrast, the RTM proposes that the nature of admixed gases will be critical to the broadening mechanism that results in the observed hydrogen emission profile. This aspect is

tested by mixing different gases with hydrogen and observing broadening in the plasma emission profile. In addition to plasma emission spectroscopy, a Langmuir probe is also used to diagnose the capacitive discharge plasma. It should be noted here that the experiments were designed and parameter regimes were considered primarily to test the field acceleration based Collisional Model (CM). In this process, however, the Resonance Transfer Model (RTM) is also tested in light of these new observations.

II. EXPERIMENTAL SYSTEM

The experimental arrangement of the DC discharge is shown in Figure 1. In this configuration, the discharge is created between fine tips of 2% thoriated tungsten electrodes of diameter 1/8 inch spaced 2 cm apart inside either a ½ inch or 1 inch diameter quartz tube. Very fine electrode tips (Fig.1) that are tapered over the last ½ inch to a point are used to minimize the surface area perpendicular to the face of the electrodes. The high E-field near the sharp electrode tip will reduce rapidly as one moves away from it. High-resolution plasma emission spectroscopy is performed through an annulus parallel to the electrode axis along the electric field lines (end-on) and perpendicular to the field lines (side-on). For the end-on observation, plasma emission can be sampled looking towards the anode or cathode. For the side-on observation, an axial scan of the plasma emission is observed in a region adjacent to the cathode rod. Here the cathode tip is located at z=0 cm. The DC plasma setup is placed on an X-Y motion table so that an accurate axial measurement can be carried out without changing the position of the fiber optic bundle. The discharge pressure is maintained in the range of 10 mTorr to 10 Torr. A stabilized negative DC power supply (Kaiser System Inc., Beverly, MA) with voltage and current in the range 0-2000 V and 0-500 mA, respectively, is used to create the plasma. A high

wattage ballast resistor of 20 kΩ is used in series with the power supply to limit the discharge current. Once the discharge is created, the glow discharge is maintained with cathode-anode voltages of 300-400 volts and results in discharge currents in the range of 10-100 mA depending upon the gas pressure, gas flow and discharge configuration.

The capacitively driven radio frequency plasma system consists of a large cylindrical (14 cm ID × 36 cm length) quartz plasma chamber with two electrodes (stainless steel plates of diameter 8.25 cm) placed 1 cm apart at the center (Figure 2). Radio frequency power (13.56 MHz, RF Power Products Inc. NJ, Model RF 5, 500 Watts) is coupled to the electrode using a commercially available impedance matching network (RF VII Inc., Glassboro, NJ). Radio frequency power from the source is fed through the impedance matchbox to the capacitive electrodes using a 1/2-inch diameter steel tube that also facilitates the end-on (parallel to the electric field) observation of plasma through holes in the center of the electrodes. One of the electrodes is permanently grounded. A common ground is maintained for the grounded electrode, rf shield and vacuum system. Two ports in the center of the plasma chamber (Position 2) permit side-on observations of plasma emission 90° and 45° to the electric field. Another side port at the same position allows insertion of a Langmuir probe for plasma density and electron temperature measurements. Plasma emission far away (15 cm) from the high-field plasma sheath region is sampled at Positions 1 and 2. In order to ensure that the plasma emission sampled at positions 1 and 2 have no contribution from the reflected light, the inside of the rf shield enclosure is made non-reflecting.

A helium leak detector (QualyTest, Model: HLT 260, Pfeiffer Vacuum) is utilized to leak test the evacuated plasma chamber. The plasma chamber is maintained with a leak rate below 10^{-7} Torr-L/s. Independent mass flow controllers (MKS) were used to introduce UHP grade

(99.999%) H_2, Ar, He and Xe gases into the plasma chamber through Ultratorr fittings at one end. The chamber pressure for all gas compositions is maintained between 10 mTorr and 10 Torr. An MKS Baratron gauge is used to read the chamber pressure.

III. DIAGNOSTICS

A. Plasma Emission Spectroscopy

Plasma emission from the glow discharge passes through a high-quality UV (200-800 nm) fiber-optic bundle into a monochromator through a 220F matching fiber adapter that is detected either by a photomultiplier tube (PMT) with a stand-alone power supply of 995 volts or by a high quality scientific grade liquid nitrogen cooled CCD arrays. The numerical aperture of the fiber optic bundle is 0.12 and the corresponding acceptance angle is 12^0. The spectrometer utilizes a 1250 mm focal length spectrometer (Jobin Yvon Horiba: Model 1250M Research Spectrometer) with a 2400 g/mm grating and a high resolution of ± 0.006 nm. The spectrometer is rated for an accuracy of ±0.05 nm and repeatability of ±0.005 nm. The spectrometer was scanned through emission profiles of Balmer lines with a step size of 0.01 nm. The entrance and exit slits were set at 20 μm. The liquid nitrogen cooled Symphony model CCD detectors are a family of array detectors from Jobin Yvon with 16 bit ADC with 20 KHz and 1 MHz read out. A back illuminated 2048×512 CCD of 13.5 μm × 13.5 μm size provides very high-resolution capability.

The Doppler-broadened line shapes for atomic hydrogen have been used to calculate the energy of the atomic hydrogen. The motion of a radiating particle moving towards or away from an observer results in a wavelength shift of the emitted line. This broadening is related to the random thermal motion of the emitting atoms and for a Maxwellian velocity distribution it

depends only on the translational (kinetic) temperature. Full half-width, $\Delta\lambda_G$, of the Gaussian profile results from the Doppler ($\Delta\lambda_D$) and instrumental ($\Delta\lambda_I$) half-widths are $\Delta\lambda_G = \sqrt{\Delta\lambda_D^2 + \Delta\lambda_I^2}$. The instrumental half-width $\Delta\lambda_I$ is 0.006 nm and is negligible. The temperature of atomic hydrogen in terms of Doppler ($\Delta\lambda_D$) half-width is given as [27]

$$\Delta\lambda_D = 7.16\times10^{-7}\lambda_0\left(\frac{T}{\mu}\right)^{1/2} \text{ nm.}$$

Here λ_0 is the line wavelength in nm, T is the temperature in K, and μ is atomic mass number(=1 for hydrogen). It can be seen that Doppler broadening is more pronounced for lighter elements at high temperatures. For high densities $>10^{13}$/cc, Doppler broadening competes with Stark broadening. In addition, a contribution to the broadened profile may arise from the mass motion of the plasma. However, for these glow discharges where the plasma density is low ($<10^{11}$/cc), the contribution of Stark broadening to the line shape profile can be neglected without loss of accuracy. We checked the contribution from the mass motion of the plasma by sampling the plasma emission side-on as well as end-on. The absence of line shift shows that the line broadening is primarily due to the thermal motion. In each case, the error in the average Doppler half-width over 10 scans was about ±5% that is attributed to the fluctuations in the plasma. The half-width of the Doppler broadened emission profile was obtained using a multi-Gaussian curve fit utilizing the curve fitting software GRAMS from Jobin Yvon Horiba.

B. Plasma Density Measurement

In the present work, Langmuir probe (LP) data has been used for obtaining the bulk plasma density and bulk electron temperature in the capacitive discharge [28-29]. The cylindrical Langmuir probe is a tungsten tip of radius 1 mm and length 5 mm enclosed in an alumina tube.

The LP is placed between the electrodes at position 2 where most of the plasma heating occurs. In order to characterize the capacitively coupled radio frequency plasma, an rf compensated LP is utilized that allows accurate measurement of bulk electron temperature. The probe filtering does not allow time varying, non-Maxwellian properties of the electron energy distribution to be readily observed. Thus, the possible presence of a small population of hot electrons ($E_c > 20$ eV) in such low-density capacitive discharges at gas pressures above 10 mTorr is not considered in this paper. Data acquisition software written in Lab View is used for automatic transfer from the oscilloscope to the computer. The entire LP data analysis in the present work was undertaken using an interactive graphics based software package developed in MatLab.

IV. EXPERIMENTAL RESULTS

A. DC Discharge

The axial profile of the Balmer H_α line (near 656.3 nm) observed perpendicular (side-on) and parallel to the electrode axis (end-on) looking towards anode as well as cathode is obtained for 1 Torr of Ar/H_2 (95/5%), He/H_2 (95/5%), and Xe/H_2 (95/5%) 300-400 V DC plasmas produced between fine tipped electrodes spaced 2 cm apart. The DC discharge is produced over a wide pressure range (and ion mean free path) of 10 mTorr-10 Torr. Significant broadening was observed for Ar/H_2 and He/H_2 plasmas whereas no broadening was observed for Xe/H_2 plasmas.

Axial profiles of the H_α line for side-on as well as for end-on observations for 1 Torr argon mixed with 5% hydrogen plasma are shown in Fig. 3 and Fig. 4, respectively. The emission profile is isotropic and symmetric. The axial scan is performed parallel to the cathode pin axis with the tip located at z=0. The fiber optic cable entrance aperture is placed perpendicular to the surface of the quartz tube. The sampled plasma volume with an acceptance

angle of 12^0 for 1 inch and ½ inch diameter tubes is 30 mm^3 and 4 mm^3, respectively. The H_α line profiles clearly exhibit a two-component Doppler-broadened profile corresponding to two populations of hydrogen atoms. The central narrow part corresponds to slow hydrogen atoms with temperatures in the range of 0.4-0.5 eV. The broad component of the profile corresponds to fast hydrogen atoms with an average temperature of ~ 40 eV. The fractional concentration of the slow part as obtained by curve fitting is 20-25% and the fast hydrogen component corresponds to 80-75 % indicating that the production of fast hydrogen atoms is substantial. Similar emission profiles are obtained for He/H_2 plasmas where the fast hydrogen atoms have temperatures in the range of 30-40 eV. In contrast, only the slow component (~0.5 eV) of the hydrogen population is observed for Xe/H_2 plasmas (Fig. 5). The axial temperature and population profiles of both fast and slow hydrogen atoms corresponding to the emission profiles in Fig.3 are shown in Fig. 6. It can also be seen from Figs. 3 and 6 that the average width of the two Gaussians of the Doppler broadened profile and hence the average temperature does not change appreciably along the axis. Even though the potential drops primarily near the cathode tip, the population of fast hydrogen atoms (area under the curve) peaks at a distance 2 cm away from the cathode tip. Moreover, the population of fast hydrogen atoms as a fraction of the total population is a minimum (82%) at the cathode tip (z=0) and it increases to 94% at z = 2 cm and remains nearly uniform up to z = 8 cm (Fig. 6). It is noted that the intensity and corresponding plasma density decreases away from the cathode tip (Fig. 3) although the hot hydrogen component increases.

Figure 7 shows the normalized emission profile for an end-on observation in Ar/H_2 and He/H_2 plasmas looking towards the anode. A similar symmetrical emission profile is also obtained when the emission is sampled looking towards the cathode. Reflection of field-accelerated ions in equal measure to the accelerated direction is required by the CM to explain

the absence of either a predominant red or blue wing in the emission profile for the end-on observation. Furthermore, the symmetrical profile cannot be explained by the gas matrix collision effect as no change in the normalized profile symmetry is observed as the gas pressure is varied from 10 mTorr to 10 Torr resulting in a variation of electron-neutral collision frequency by three orders of magnitude (Fig. 8).

The average thermal energy of hot hydrogen atoms as catalytic (Ar, He) and non-catalytic (Xe) gases are added to a 100 mTorr hydrogen plasma DC discharge is shown in Fig. 9. As the fractional concentration of the catalyst gas is increased, the thermal energy of hot hydrogen atoms increases. In contrast, the hot H atom thermal energy decreases sharply with increasing Xe concentration. The absence of H_α broadening with a non-catalyst such as Xe cannot be explained on the basis of the collisional model since the acceleration mechanism should be independent of the ion mass.

In addition, the transfer of energy from the electric field in these admixed plasmas is selectively to hydrogen atoms. Since the mass ratio of He to atomic hydrogen is 4:1, especially for highly collisional plasmas at higher gas pressures, it is expected from the Collisional Model [5] that a correspondingly energetic concentration of helium atoms (Doppler broadened profile) will be present. The Doppler half-width of the 667.82 nm He I line as shown in Fig. 10 is 0.012 nm and it can be accurately resolved by the high-resolution spectrometer with an instrumental half-width of only 0.006 nm. The He atoms' average thermal energy corresponding to a 0.012 nm Doppler half-width is 0.2 eV. No change in Doppler broadening of the 667.82 nm He I line was observed for all pressure and composition ranges studied in these experiments. The absence of hot helium atoms in He/H_2 plasmas where the hydrogen atoms have 30-40 eV energies also contradicts the Collisional Model because the atomic mass ratios are comparable (4:1).

B. Capacitively Coupled RF Discharge

The capacitively coupled radio frequency discharge is characterized using Langmuir probe (LP) and plasma emission spectroscopy diagnostics. The LP is employed to measure electron bulk plasma density (n_e) and electron temperature (T_e) and to determine if a bulk population of high temperature (>5 eV) electrons, not detectable by spectroscopic techniques, exists in our capacitively coupled RF plasmas. A side port at position 2 (Fig. 2) allows the insertion of the LP between the rf electrodes. The on-axis LP measurements are summarized in Table 1 for different noble gases admixed with 10% hydrogen at constant pressure of 100 mTorr. The coupled radio frequency power is maintained constant at 100 W for all the cases. In general, a low-density plasma (~10^{10} cm^{-3}) with bulk electron temperatures of 2-3 eV is observed for all plasma conditions. There is a slight drop (~15-20%) in n_e as well as in T_e as hydrogen is added to the pure noble gas plasmas. It should be noted, however, that we did not observe any high-energy (>5 eV) electron population obtained from the LP measurements. A single temperature bulk electron population characterizes these plasmas. The absence of higher-energy electrons in the higher-field regions between the electrode plates implies that there also are no fast electrons in low field regions far away from the electrodes.

Plasma emission from capacitively coupled rf discharges varied over a wide pressure range is sampled perpendicular to the electric field between the large disc electrodes (Position 2 in Fig. 2) and along the electric field through the 1 cm holes in the electrode plates (end-on). In addition, observations are also made at locations far way from the electrode plates (Positions 1 and 3 in Fig. 2). Isotropic and symmetric H_α line profiles are observed for all three locations, independent of the observation angle relative to the electric field direction. The line profile also

remains symmetric as the gas pressure is varied over a wide range from 10 mTorr to 10 Torr. Line broadening is observed only for Ar/H_2 and He/H_2 plasmas and there is no broadening in comparable control mixtures of Xe/H_2. The energy of the hot H atoms increases with increasing concentration of Ar and He gases whereas it decreases with Xe concentration. For the Ar/H_2 and He/H_2 plasmas the energy is selectively transferred to hydrogen atoms. In addition, the temperature of fast H atoms is quite uniform throughout the plasma chamber.

The average thermal energy of hot hydrogen atoms as a function of Ar, He and Xe concentrations [H_2(x sccm); Ar, He, Xe (y=1-x sccm)] is shown in Fig. 11. A pure hydrogen plasma at 150 mTorr with a 20 sccm flow rate is produced at a coupled rf power level of 200 W. The corresponding thermal energy of the fast hydrogen atoms in this hydrogen plasma is ~ 13-15 eV. Noble gases are introduced into the plasma chamber and the total chamber pressure and flow rate are maintained at 150 mTorr and 20 sccm, respectively, by adjusting the hydrogen and noble gas flow rates. As shown in Fig. 11, the average thermal energy of the hydrogen atom, obtained from symmetric emission profiles, increases from ~13-15 eV to 25-30 eV as the Ar and He fraction is increased. In contrast, the average energy of the hydrogen atom decreases with increasing concentration of Xe.

Figures 12 and 13 show the energy and fractional population of fast hydrogen atoms in Ar/H_2 (95/5%) plasmas as the chamber pressure is varied from 10 mTorr to 10 Torr. Plasma emission is sampled perpendicular to the field between the electrodes and along the field lines through holes in the powered and grounded electrodes. As shown in the figures, the fast hydrogen energy (20-25 eV) and their fractional population (70-80%) in n=3 states remains nearly constant as the gas pressure is varied over three orders of magnitude. Very similar profiles

of fast hydrogen energy (Fig. 14) and fractional population (Fig.15) as a function of pressure are obtained for (95/5%) He/H_2 plasmas.

The presence of hot hydrogen far away from the high field sheath region is in contradiction with the Collisional Model. The plasma emission is sampled at Position 1 and Position 3 (Fig. 2) and angular variation is obtained by rotating the optical probe. The reference is normal to the chamber axis and as the observation angle is varied, plasma emission far away (~ 6 cm) from the electrode region is sampled. As shown in Fig. 16, there is a very small influence of the tilt angle on the hot hydrogen energy for both Ar/H_2 and He/H_2 plasmas. It should be noted here that the symmetry of the emission profile is independent of the angle of observation.

V DISCUSSION

The observations and implications resulting from this study contradict the Collisional Model [5] where excessive H_α broadening in pure hydrogen and mixtures of hydrogen with noble gases is explained primarily in terms of energetic ions (H^+, H_2^+ and H_3^+) accelerated in the cathode fall region followed by energy transfer to the matrix gas (H and H_2) through charge exchange collisions. The character of atomic hydrogen broadening, namely the fast component temperature and the fractional population of the fast hydrogen atoms is quite different for different gas mixtures. In all variations of the collisional model [5], one consistent aspect is that the energy required for selective heating of the hydrogen atoms in plasmas consisting of hydrogen and hydrogen admixed with other gases is locally absorbed by ions from the electric field in the cathode fall region. In the CM at low pressures and collisionality, the emission profile should be dependent on the observation angle relative to the electric field direction. In order to explain the observed symmetry in the emission profile, they have argued that sputtered fast H

atoms and the back-reflected fast H atoms from the cathode surface give rise to fast H concentrations leaving the cathode in the same abundance as that moving towards the cathode.

We summarize the significant results of our experimental observations that are inconsistent with the field acceleration based Collisional Model [5]: 1) Hot hydrogen atoms are observed only for pure hydrogen and specific mixtures such as Ar/H_2 and He/H_2 plasmas whereas no hot H atoms are found when hydrogen is admixed with electronically similar Xe [36]. 2) In the Ar/H_2 and He/H_2 cases, energy is transferred selectively to hydrogen atoms where molecular hydrogen and the admixed gas atoms remain colder (<0.5 eV). 3) The population of neutral H atoms is much hotter (15-40 eV) than any of the charged species ($T_e \sim$ 2-3 eV in capacitive discharge). 4) The emission profile is symmetric over a wide pressure and mean free path range (three orders of magnitude) and is independent of the observation angle relative to the electric field direction. 5) Comparably hot hydrogen atoms are observed in field-free regions far away (up to 15 cm) from the high-field sheath region. In the following sections we discuss the inconsistency of the field acceleration based Collisional Model to account for these results and demonstrate that the Resonance Transfer Model is consistent with these observations.

Let us consider the presence of hot hydrogen atoms that occur only for pure hydrogen and hydrogen admixed with Ar and He plasmas and the absence of hot hydrogen atoms in electronically similar Xe/H_2 plasmas for the entire pressure range from 10 mTorr to 10 Torr. In the field acceleration based Collisional Model, the energy of hot hydrogen atoms should be independent of the nature of the electronically similar background gas except for differing collision cross sections of their ions with H. In order to test the collisional effect of background gases, we consider the cross section data for Balmer alpha and beta line emission from H and H^+ impact reactions on hydrogen (H_2) and our other reacting gases [31-36]. It should be noted that

cross-section data for low energy (< 100 eV) H and H^+ impact on all three reacting gases considered in this paper are not available. Therefore, H_α emission cross-sections from the impact of 100 eV H atoms on noble gas targets $H + X(X = Ar, He, Xe) \rightarrow H_\alpha$ are considered. These are 7×10^{-17} cm^2, 2×10^{-18} cm^2, and 5×10^{-18} cm^2 for Ar, He, and Xe, respectively, [31,33,35]. Similarly, the H_α emission cross-sections from 100 eV H^+ impact $H^+ + X(X = Ar, Xe) \rightarrow H_\alpha$, are 2×10^{-19} cm^2 and 1×10^{-17} cm^2 for Ar and Xe, respectively [32,36]. The emission cross-section data for $H^+ + He \rightarrow H_\alpha$ reaction is not available for H^+ energies below 1.25 keV because of the small magnitude of the photon signals [36]. The cross section for $H^+ + He \rightarrow H_\alpha$ collisions at H^+ energies of 1.25 keV is given as $0.6\pm0.3 \times10^{-20}$ cm^2 and it will be much smaller for lower H^+ energies [36].

The CM argues that H^+ ions will travel and be accelerated over longer distances and gain more energy before interacting with the target gas if the cross-section of H^+ impact on the target gas is smaller. As a result, increasingly energetic H^+ ions and, therefore via charge exchange, more energetic H atoms should be observed when the target gas is changed from Xe to Ar to He. Hence, following these arguments, we should observe the most energetic H atoms in the presence of He gas at low pressure. In addition, the H_α emission intensity should be similar for both He and Xe since the H impact cross-sections on He and Xe are similar. However, we observe H atoms of comparable energy (30-40 eV in the DC discharge and 20-25 eV in the capacitive discharge) with either He or Ar as the background gas whereas the H atom energies are only 1-2 eV with Xe. The H_α line intensity is also sharply reduced in Xe/H_2 discharges indicating low atomic hydrogen concentrations in non-RT plasmas. It can be concluded,

therefore, that the collisional model fails to explain the absence of fast H in Xe/H_2 discharges in contrast to its presence in Ar/H_2 and He/H_2 discharges.

These observations are consistent with the RTM which mandates that hot hydrogen atoms will be observed in Resonance Transfer (RT) plasmas where an ion is present that can provide a net enthalpy of reaction of an integer multiple of the potential energy of atomic hydrogen. Hence He^+, and Ar^+ can act as 'catalysts' for the process since the electron ionization energies are an integral multiple of 27.2 eV [24]. Furthermore, as predicted by the RTM, Xe species are incapable of acting as catalysts since the ionization energy for Xe is not an integral multiple of 27.2 eV. As a result we do not observe hot hydrogen atoms in Xe/H_2 plasmas. In addition, the atomic hydrogen concentrations in non-RT plasmas are also low as evidenced by the emission line intensity.

We now consider the observation that the energy is transferred selectively primarily to hydrogen atoms (15-40 eV) whereas the atoms of admixed gases remain cold (<0.5 eV). In the Collisional Model there are neither preferred ions nor atoms and, therefore, one should observe correspondingly hot atoms of the admixed gases along with the hot hydrogen atoms. To our knowledge, no measurement has ever been made where equally hot atoms of admixed gases have been found. In collision dominated plasmas at higher gas pressures where an ion is bound to suffer many collisions with the background gas as it moves towards the cathode and where the mass ratios of the constituent gases are comparable, the presence of correspondingly hot atoms of admixed gases is inferred from the Collisional Model. Let us consider a He/H_2 plasma at 10 Torr with the electron-neutral collision frequency of 3×10^{10} s^{-1} [30]. If in gas mixtures where only a trace amount of hydrogen (~1%) is added to the helium plasma, plasma hydrogen and helium ions will undergo many collisions with the background helium gas as they travel towards

cathode. It should be noted that the recombination rate coefficients of helium and hydrogen ions with energy in the range ≈ 20-30 eV is given by the reaction $He^+ + e \rightarrow He$ and $H^+ + e \rightarrow H$. The two-body recombination rates for these two processes are comparable (α_e=10^{-13} cm^3/s) [37-38]. Therefore, the survival probability of both He^+ and H^+ ions as they travel towards the cathode is comparable. It should be noted, however, that with an atomic mass ratio of 4:1 in helium-atomic hydrogen plasmas, we observe hydrogen atoms with average energies of 30-40 eV whereas helium atoms are cold and have energies less than 0.5 eV (Fig. 10). In contrast, this selective transfer of energy to hydrogen atoms even though other comparable mass ratio ions are present is a cornerstone of the RTM prediction.

As shown in Fig. 16, there is a significant presence of comparably hot hydrogen atoms far away from the high-field plasma sheath regions where most of the potential variation occurs. It is well known that outside the sheath region, where the plasma is largely quasi-neutral, the plasma potential variation is very small. Therefore, in a field free region, the field acceleration CM cannot explain the existence of hot hydrogen up to 15 cm from the electrode. In order to explain the presence of hot H atoms in low field regions, the modified CM [5] requires the presence of fast electrons that produce hot atomic hydrogen with an energy comparable in magnitude to that obtained in the high field region where the source of these atoms are accelerated ions in the sheath. The measured electron temperature using the Langmuir probe located between the rf plates, where most of the electron heating takes place, is ≈ 2-3 eV (Table 1). It is reasonable, therefore, to argue that the bulk of the plasma well away from the electrodes region is cold. Moreover, the tail of the electron energy distribution function comprising high-energy electrons is not observed in the LP measurements for up to – 70 V applied voltages and is definitely negligible in the region far away from the electrodes. Hence, these electrons cannot

produce energetic ions that recombine to form H atoms with energies > 15-20 eV. The cross sections for resonant charge exchange transfer ($Ar^{+}_{fast} + Ar_{slow} \rightarrow Ar_{fast} + Ar^{+}_{slow}$ and $He^{+}_{fast} + He_{slow} \rightarrow He_{fast} + He^{+}_{slow}$) can be utilized to estimate the distance traveled by an ion produced in the cathode fall region without suffering a charge exchange collision that reduces the maximum energy it can obtain. At 20 eV, the resonant charge exchange transfer cross sections (σ_i) for Ar and He ions are comparable at 2.2×10^{-15} cm^2 and 1.5×10^{-15} cm^2, respectively [39]. The mean free path is given as $\lambda_i = \frac{1}{n_g \sigma_i}$ cm, where n_g, the neutral particle density, is a function of gas pressure. At 10 mTorr, the mean-free path for charge transfer, λ_i, is 0.06 cm. Therefore, the ions produced in the cathode fall region will not maintain their energy over a distance of 15 cm without suffering a charge exchange collision in these plasmas [39]. These ions cannot be the source of hot H atoms in a region far away from the electrodes. Moreover, the radiative lifetime of the hydrogen n=3 state is 10^{-8} s [15] and with an assumed average velocity of 10^6-10^7 cm/s corresponding to hydrogen energies of 1-100 eV, it can only travel a distance of 0.01-0.1 mm before emission and reduced energy. This implies that the observed H_α emission is a result of local excitation. The rapid thermalization of H atoms with the background gas will also localize fast H concentrations to the region where it is formed. Therefore, a mechanism that explains the localized production of hot H over the larger plasma chamber is required. Mills' hypothesis of a catalytic reaction of hydrogen is consistent with the observation of hot H atoms far way from the high field region.

In order to explain the symmetric line emission profile, the CM model mandates the presence of a reflector or divertor. In this model a Gaussian distribution is achieved either by the scattering of hydrogen atoms by the electrode surface or by collisional excitation of H_f on H_2

with large angle scattering [6], where H_f represents the hot hydrogen atoms that have previously collided with the electrode. This implies that the sputtered fast H atoms and the back-reflected fast H atoms from the cathode surface are produced in equal measure to produce a symmetric profile. This requires an "ideal isotropic reflector" to reverse the momentum of a positive ion gained from the electric field to give rise to fast H leaving the cathode in the same abundance as that moving towards the cathode. In addition, according to their model, a "divertor" must also exist such that the ratio of fast H at any given energy towards and away from the cathode remains equal and this must be the case in all directions including the direction perpendicular to the electric field. The interaction of an H atom with a metal surface is quasi-elastic for a large range of targets and energies. The particle and energy reflection coefficients for hydrogen atoms to be reflected back in the energy range of 20-30 eV are only 50% [40]. Therefore, the possibility that backscattered H atoms produced with a comparable distribution to those of the incident H atoms with comparable energy distributions so as to yield a symmetric profile is not feasible. In addition, it is well known that the effective cross section for many small-angle ion-neutral collisions to produce an equivalent deflection is larger than that for single large-angle collision [41]. Hence, this argument is not viable as a mechanism to explain the symmetry of the plasma emission profile.

Electron-ion, electron-neutral, and ion-neutral collision frequencies are a complex function of not only the gas pressure but also of the energy of the colliding particles. Therefore, in order to obtain a better insight into the energy transfer through the collision and charge exchange process, an estimate of the collision frequencies at the pressure and energies of interest is discussed. For a flux of incident electrons with velocities v colliding with a background neutral gas, the collision frequency is given approximately as $\nu_{cn} = n_g \sigma v = n_g K \sim 3 \times 10^9 \times P(\text{Torr}) s^{-1}$

where n_g is the neutral number density given by Loschmidt's number and σ is the collision cross-section and K is the rate constant [41-42]. At 10 mTorr and 10 Torr, the electron-neutral collision frequencies are 3×10^7 s^{-1} and 3×10^{10} s^{-1}, respectively, a variation of three orders of magnitude. Therefore at 10 mTorr, the electron-neutral collision frequency is comparable to the rf frequency and the electron can travel to the anode in one rf period of 73 ns. The LP measured electron temperature is 2-3 eV and the electron can travel a distance of about 8 cm during one rf period without suffering collisions with the background neutral gas. Therefore, in low-collision-rate plasmas compared to the ion transit time between the electrodes, based on the CM, fast H atoms produced by the charge exchange process will continue to move towards the direction of the accelerated ions and will yield a predominant red or blue wing in the emission spectrum relative to the direction of observation. However, the data presented in this paper are contrary to the prediction of the CM field acceleration mechanism of energy transfer to hydrogen atom. The symmetric line profile is independent of the angle of observation.

VI CONCLUSION

The mechanism of extraordinary broadening of the hydrogen Balmer lines in hydrogen admixed with noble gases has been studied in two different discharge systems over a wide parameter range to examine highly collisional and weakly collsional regimes. Experiments were performed to test the validity of the field acceleration based Collisional Model. The field acceleration based Collisional Models were formulated to explain the energy gained by hydrogen atoms in experiments where only hydrogen plasmas and plasmas of hydrogen admixed with much heavier noble gases (Ar) were considered. As a result, the selective transfer of energy only to the hydrogen atom was not considered while theories were formulated to explain the

extraordinary broadening. However, we have found that energy is transferred only to hydrogen atoms and not to the admixed gases even when the admixed gas is helium with a mass ratio of 4:1. It was also realized that this energy transfer is not the same even when the admixed gases are electronically similar. For example, hot H atoms are absent when He and Ar are replaced with an electronically similar noble gas Xe. The directionality of energy gained according to the field acceleration based CM mechanism was tested by using sharp tipped electrodes in a DC discharge, thus minimizing the electrode surface area perpendicular to the axis. The plasma emission parallel and perpendicular to the electric field lines was sampled over a wide pressure range. The H_α line profiles were observed to be symmetric in all cases. As discussed earlier, this symmetry can not be explained by the field acceleration based CM model, including its variations where it is argued that equally hot H atoms in equal measure are produced by backscattering with the cathode surface.

Moreover, the Collisional Model utilizes the presence of a plasma sheath where most of the ions are accelerated and these then transfer energy to hydrogen atoms through the charge exchange process. It has been shown in this paper that hot hydrogen atoms are observed far away from the cathode fall regions in plasmas. The presence of hot H in a region where the plasma potential variation is low and plasma electrons are cold (T_e<2 eV), is clearly in contrast to the CM. It is concluded that these observations are consistent with the RT-plasma mechanism.

References:

1. A.L. Cappelli, R.A. Gottscho, and T.A. Miller, "Doppler-broadened line shapes of atomic hydrogen in a parallel-plate radio frequency discharge," *Plasma Chem. Plasma Process*, vol. 5, pp. 317-331, 1985.
2. G. Baravian, Y. Chouan, A. Ricard, and G. Sultan, "Doppler broadened H_α line shapes in a rf low pressure H_2 discharge," *J. Appl. Phys.*, vol. 61, pp. 5249-5253, 1987.
3. S. Djurovic and J.R. Roberts, "Hydrogen Balmer alpha line shapes for hydrogen-argon mixtures in a low-pressure rf discharge," *J. Appl. Phys.*, vol. 74, pp. 6558-6565, 1993.
4. C. Barabeau and J. Jolly, "Spectroscopic investigation of energetic atoms in a DC hydrogen glow discharge," *J. Phys. D, Appl. Phys.*, vol. 23, pp. 1168-1174, 1990.
5. N. Cvetanovic, M. M. Kuraica, and N. Konjevic, "Excessive Balmer line broadening in a plane cathode abnormal glow discharge in hydrogen," *J. Appl. Phys.*, vol. 97, pp. 33302-33309, 2005.
6. M.R.G. Adamov, B.M.Obradovic, M.M. Kuracia, and N. Konjevic, "Doppler spectroscopy of hydrogen and deuterium Balmer alpha line in an abnormal glow discharge," *IEEE Trans. Plasma Sci.*, vol. 31, no. 3, pp. 444-454, 2003.
7. E. L. Ayers and W. Benesch, "Shapes of atomic-hydrogen lines produced at cathode surface," *Phys. Rev. A, Gen. Phys.*, vol. 37, pp. 194, 1988.
8. W. Benesch and E. Li, "Line shapes of atomic hydrogen in hollow cathode discharge," *Opt. Lett.*, vol. 9, no. 8, pp. 338-340, 1984.
9. M. Kuraica and N. Konjevic, "Line shapes of atomic hydrogen in a plane-cathode abnormal glow discharge," *Phys. Rev. A*, vol. 46, no. 7, pp. 4429-4432, 1992.
10. M. Kuraica, N. Konjevic, M. Platisa, and D. Pantelic, "Plasma diagnostics of the Grimm-

type glow discharge," *Spectrochim. Act,* vol. 47, pp. 1173, 1992.

11. S. Alexiou and E. Leboucher-Dalimier, "Hydrogen Balmer-α in dense plasmas," *Phys. Rev. E,* vol. 60, no. 3, pp. 3436-3438, 1999.
12. S. B. Radovanov, J. K. Otthoff, R. J. Van Brunt, and S. Djorovic, " Ion kinetic-energy distribution of Balmer-alpha (H_α) excitation in Ar-H_2 radio-frequency discharges," *J. Appl. Phys.*, vol. 78, pp. 746-757, 1995.
13. A. V. Phelps, "Collisions of H^+, H^+_2, H^+_3, ArH^+, H^-, H, and H_2 with Ar and of Ar^+ and ArH^+ with H_2 for Energies from 0.1 eV to 10 keV," *J. Phys. Chem. Ref Data,* vol. 21, pp. 883-897, 1992.
14. S. B. Radovanov, K. Dzierzega, J. R. Roberts, and J. K. Olthoff, "Time resolved Balmer-alpha emission from fast hydrogen atoms in low pressure, radiofrequency discharges in hydrogen," *Appl. Phys. Lett.*, vol. 66, no. 20, pp. 2637-2639, 1995.
15. A. Bogaerts and R. Gijbels, "Effects of adding hydrogen to an argon glow discharge: Overview of some relevant processes and some quantitative explanations," *J. Anal. At. Spectrom.*, vol. 15, pp. 441-449, 2000.
16. R. L. Mills, P. Ray, B. Dhandapani, R. M. Mayo, and J. He, "Comparison of excessive Balmer α line broadening of glow discharge and microwave hydrogen plasmas with certain catalysts," *J. Appl. Phys.*, vol. 92, pp.7008-7022, 2002.
17. R. L. Mills, P. C. Ray, M. Nansteel, X. Chen, R.M. Mayo, J. He, and B. Dhandapani, "Comparison of excessive Balmer α line broadening of inductively and capacitively coupled RF, microwave, and glow discharge hydrogen plasma with certain catalysts", *IEEE Trans. Plasma Sci.*, vol. 31, pp. 338-355, 2003.
18. R. L. Mills and P. Ray, "Extreme ultraviolet spectroscopy of helium-hydrogen plasma," *J.*

Phys. D: Appl. Phys., vol. 36, pp. 1535-1542, 2003.

19. R. L. Mills, P. Ray, B. Dhandapani, M. Nansteel, X. Chen, and J. He, " New power source from fractional quantum energy levels of atomic hydrogen that surpasses internal combustion," *J Mol. Struct*, vol. 643, no. 1-3, pp. 43-54, 2002.
20. R. Mills and P. Ray, "Spectral emission of fractional quantum energy levels of atomic hydrogen from a helium-hydrogen plasma and the implications for dark matter," *Int. J. Hydrogen Energy*, vol. 27, no. 3, pp. 301-322, 2002.
21. C. Chen, T. Wei, L. R. Collins, and J. Phillips, "Modelling the discharge region of a microwave generated hydrogen plasma." *J. Phys. D: Appl. Phys.*, vol. 32, pp. 688-698, 1999.
22. R. L. Mills and P. Ray, "Substantial changes in the characteristics of a microwave plasma due to combining argon and hydrogen," *New J. Phys.*, www.njp.org, vol. 4, pp. 22.1-22.17, 2002.
23. R. Mills, M. Nansteel, and P. Ray, "Argon-hydrogen-strontium discharge light source," *IEEE Trans. Plasma Sci.*, vol. 30, no. 2, pp. 639-652, 2002.
24. R. Mills, M. Nansteel, and P. Ray, "Bright hydrogen-light source due to resonant energy transfer with strontium and argon ions", *New J. Phys.*, vol. 4, pp. 70.1-70.28, 2002.
25. R. Mills, "Spectroscopic identification of a novel catalytic reaction of atomic hydrogen and hydride ion product", *Int. J. Hydrogen Energy*, vol. 26, pp. 1041-1058, 2001.
26. R. Mills and P. Ray, "Vibrational spectral emission of fractional-principal-quantum-energy-level hydrogen molecular ion, *Int. J. Hydrogen Energy*, vol. 27, pp. 533-564, 2002.
27. W.L. Wiese, "Line Braodening", in Plasma Diagnostic Techniques, R. H. Huddleston and S. L. Leonard, Eds., Academic Press, NY, (1965)

28. F. F. Chen, "Electric Probes", in Plasma Diagnostic Techniques, R. H. Huddleston and S. L. Leonard, Eds., Academic Press, NY, (1965).

29. A. Ganguli, M.K. Akhtar, and R.D. Tarey, "Investigation of microwave plasmas produced in a mirror machine using ordinary-mode polarization", Plasma Sources Science & Technol. 8, pp. 519, 1999.

30. Kamran Akhtar, John E. Scharer, Shane Tysk and Enny Kho," Plasma interferometery at high pressures", Rev. Sci. Instrum., 74, pp. 996, 2003.

31. B. Van Zyl, H. Neumann, H.L. Rothwell, Jr., and R.C. Amme, "Balmer-α and Balmer-β emission cross sections for H + Ar collisions", Phys. Rev. A , Vol. 21, pp. 716, 1980.

32. B. Van Zyl, H.L. Rothwell, Jr., and H. Neumann, "Balmer-α and Balmer-β emission cross sections for H^+ + Ar collisions", Phys. Rev. A , Vol. 21, pp. 730, 1980.

33. B. Van Zyl, M. W. Gealy, and H. Neumann, " Balmer-α and Balmer-β emission cross sections for low-energy H collisions with He and H_2", Phys. Rev. A, Vol. 28, pp. 176, 1983.

34. B. Van Zyl, M. W. Gealy, and H. Neumann, "Excitation of low-energy H atoms in H+Ne collisions", Phys. Rev. A , Vol. 31, 5, pp. 2922, 1985.

35. B. Van Zyl, H. Neumann, and M. W. Gealy, "Balmer-line emission from low-energy H impact on Kr and Xe", Phys. Rev. A , Vol. 33, pp. 2093, 1986.

36. B. Van Zyl, M. W. Gealy, and H. Neumann, "Balmer-line emission from low-energy H^+ impact on rare-gas atoms", Phys. Rev. A , Vol. 33, 4, pp. 2333, 1986.

37. M. Arnaud and R. Rohenflug, Astron. & Astrophys. Suppl. 60, 425 (1985),

38. T. Kato and E. Asano, " comparison of recombination rate coefficients given by empirical formulas for ions from hydrogen through nickel", NIFS-DATA-54, National Institute of Fusion Science (NIFS), Nagoya, Japan, 1999.

39. E.W. McDaniel, J.B.A. Mitchell, and M.E. Rudd, Atomic Collision: Heavy Particles Projectiles, Wiley, New York, 1993.

40. D.E. Post and R. Behisch, Physics of Plasmas-Wall Interactions in Controlled Fusion, NATO ASI series B, 131, 423, (1986)

41. M.A. Lieberman and A.J. Lichtenberg, "Principles of plasma discharges and material processing", 2nd edition, Hoboken, New Jersey: John Wiley & Sons, Inc., 2005.

42. V. Vahedi, R. A. Stewart, and M. A. Lieberman, "Analytic model of the ion angular distribution in a collisional sheath," J. Vac. Sci. Technol. A, vol. 11, pp. 1275-1282, 1993.

TABLE I

Langmuir probe measurement of plasma density and electron temperature in capacitively coupled radio frequency plasmas at 100 mTorr and 100 W coupled rf power.

Gas Composition	Bulk Plasma Density (cm^{-3})	Bulk Electron Temperature (eV)
Ar	$2\text{-}3\times10^{10}$	2.1-2.4
Ar/10%H_2	$5\text{-}8\times10^{9}$	1.8-2.0
He	$6\text{-}9\times10^{9}$	2.5-3.0
He/10%H_2	$3\text{-}5\times10^{9}$	1.9-2.3
Xe	$2\text{-}5\times10^{10}$	1.7-2.0
Xe/10%H_2	$7\text{-}9\times10^{9}$	1.7-1.9

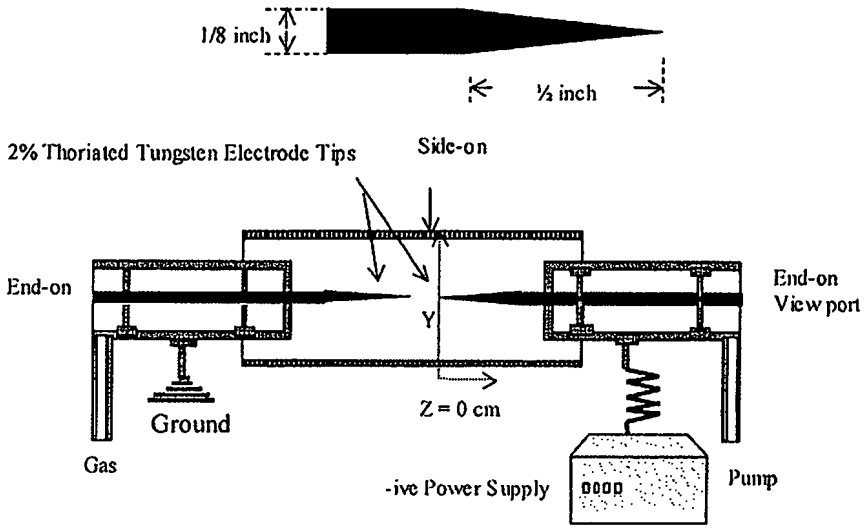

Fig 1. Schematic of the DC discharge created between the fine tips of 2% thoriated tungsten electrodes with the direction of axial scans defined. The cathode tip is taken as z=0 cm for side-on observations measured along the axis of the cathode from its tip to its electrical connection.

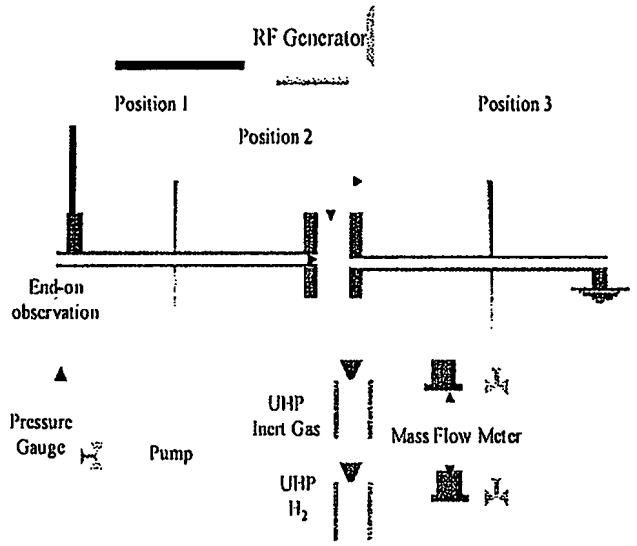

Fig.2: Schematic of the capacitively coupled radio frequency plasma system. Optical emission spectroscopy is performed perpendicular to the electric field (Position 2) and parallel to the field (end-on observation).

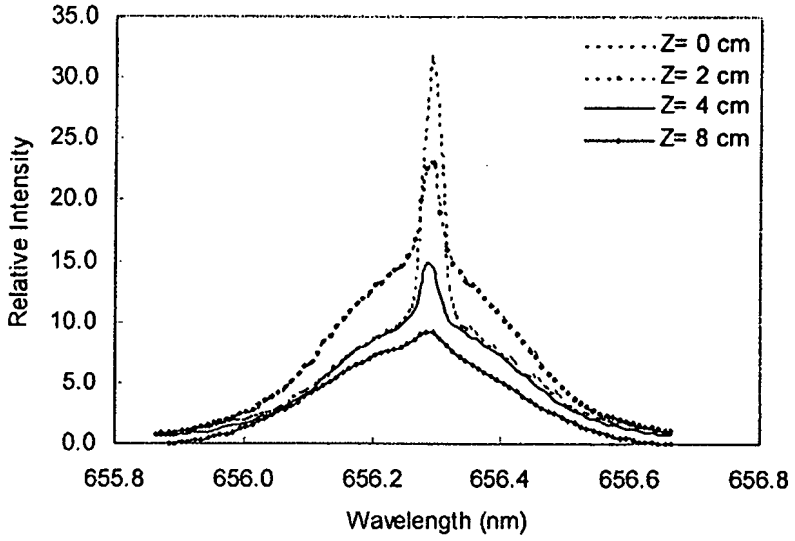

Fig. 3. Axial scan of the 656.3 nm Balmer α line width recorded on a 1 Torr *Ar* /H_2 (95/5%) DC plasma discharge with needle-like electrodes at 400 V and 20 mA showing 80% of the hydrogen was 'hot' with an average hydrogen atom energy of 40 eV, compared to < 0.5 eV for the slow population.

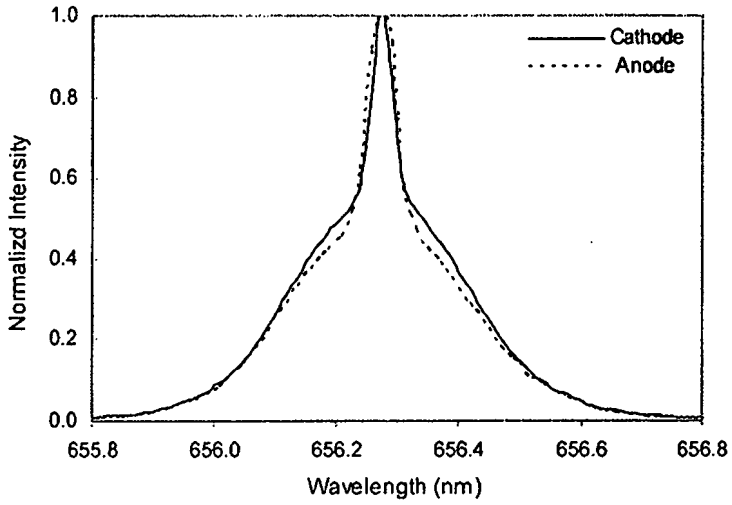

Fig. 4. The 656.3 nm Balmer α line width recorded end-on (parallel to the electric field) on a 1 Torr *Ar* /H_2 (95/5%) DC plasma discharge with needle-like electrodes at 400 V and 20 mA. Both views looking towards the cathode as well as the anode show a symmetrical emission profile. The temperature of hot hydrogen atoms is in the range of 38-40 eV.

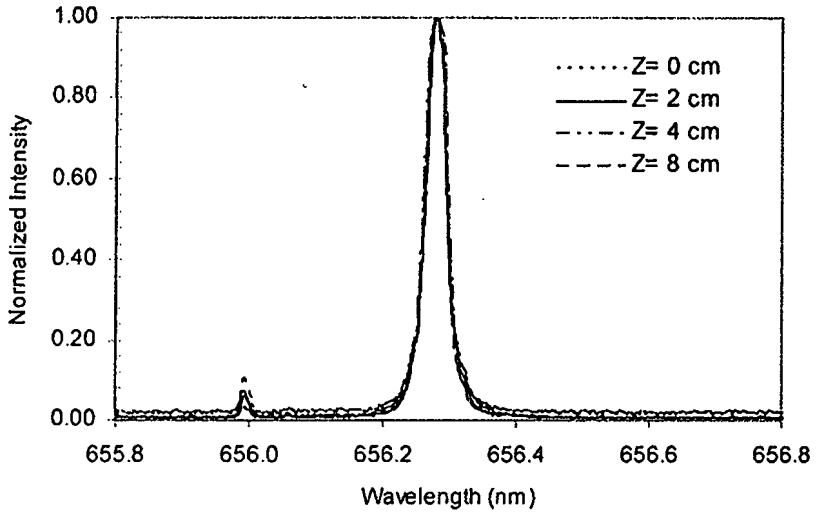

Fig. 5. Axial scan of the 656.3 nm Balmer α line width recorded on a 1 Torr *Xe* /H_2 (95/5%) DC plasma discharge with needle-like electrodes at 400 V and 20 mA showing only a cold population of <1 eV with a decrease in intensity along the cathode due to a decrease in electron density and energy.

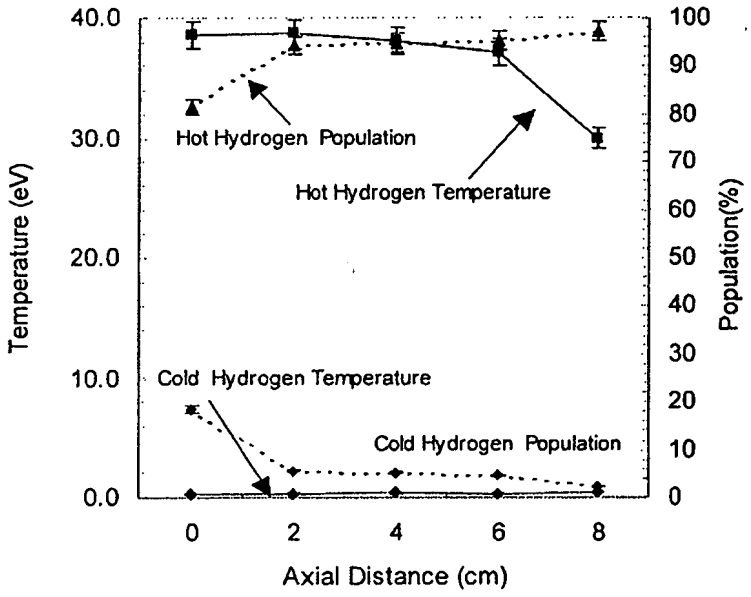

Fig. 6. Axial plots of hot hydrogen atoms temperature and population (given by area under the curve) corresponding to the spectrum in Figure. 3. A hot hydrogen population is present even at a distance of 8 cm away from the cathode tip where most of the potential falls.

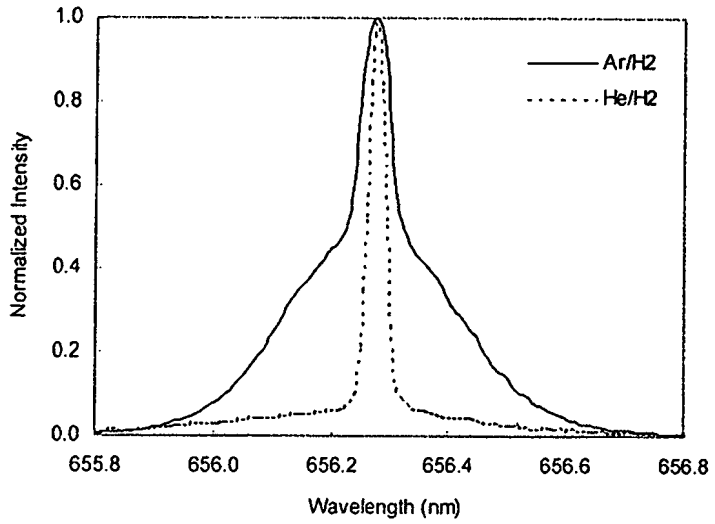

Fig. 7 Normalized end-on emission spectrum of 1 Torr Ar/5%H_2 and He/5%H_2 plasma looking towards the anode. Note the symmetrical emission profile.

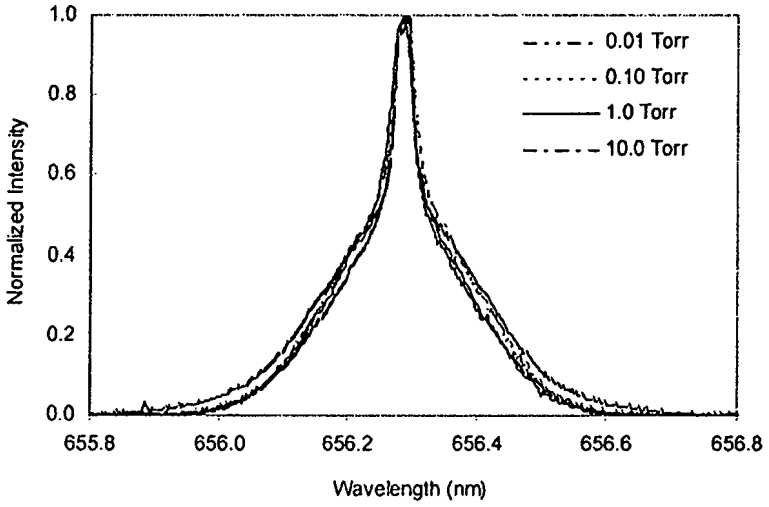

Fig. 8 Normalized end-on emission spectrum of Ar/5%H_2 plasma looking towards cathode as the gas pressure is varied over three-orders-of magnitude from 10 mTorr to 10 Torr. Note the symmetrical emission profile.

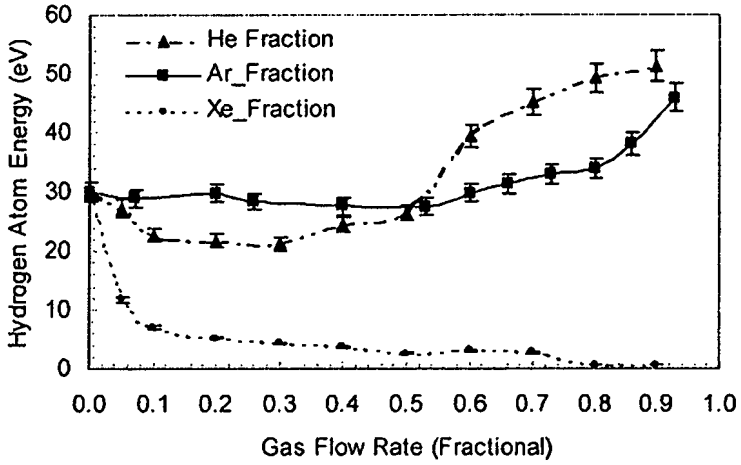

Fig.9 Energy of hot hydrogen atoms as a function of fractional concentration of admixed gases in a DC discharge at 100 mTorr. Note the increase in the energy of hot H as Ar and He concentration increases and decrease in energy with the addition of Xe.

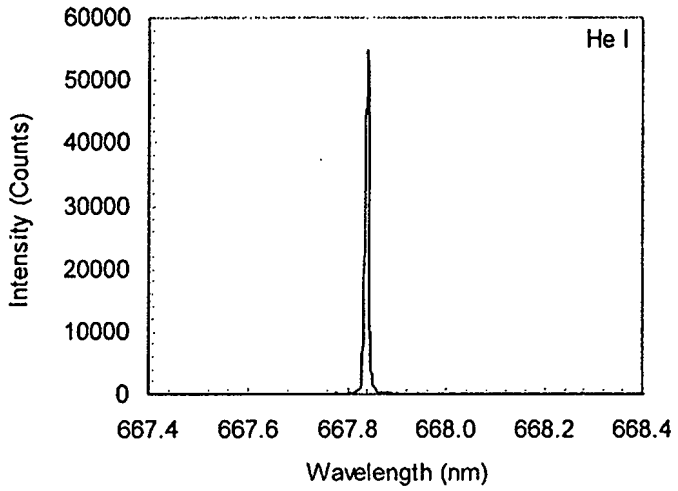

Fig. 10

Fig. 10 The 667.816 *nm* He I line width for 1 Torr He/H_2 (95/5%) at 400 V and 20 mA . No broadening was observed,

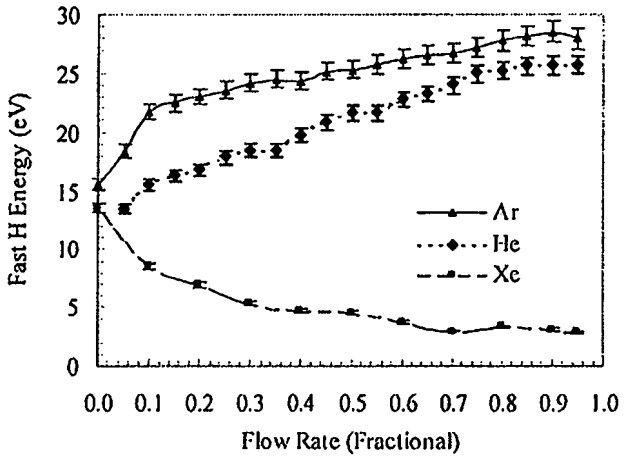

Fig.11. Energy of hot hydrogen atom in Ar/H_2, He/H_2 and Xe/H_2 plasmas as a function of the noble gas concentration [H_2(x) Ar, He, Xe(y=1-x)] in capacitively coupled rf discharge. The plasma chamber is maintained at 150 mTorr with a total flow rate of 20 sccm. The coupled rf power is 200 Watt. H_α emission is sampled perpendicular to the electric field between the capacitive plates.

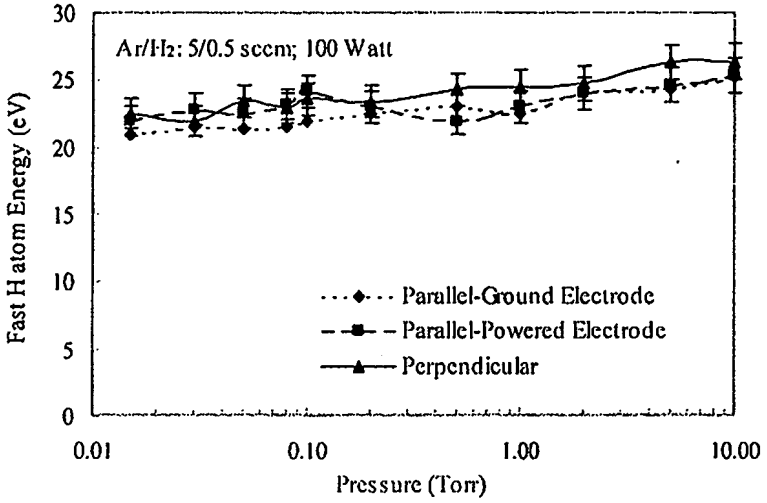

Fig. 12: Hot hydrogen atom temperature for capacitively coupled Ar/H_2 discharge at different gas pressures. Observations are made perpendicular to the field between the electrodes and parallel to the field lines through holes in both powered and grounded electrodes.

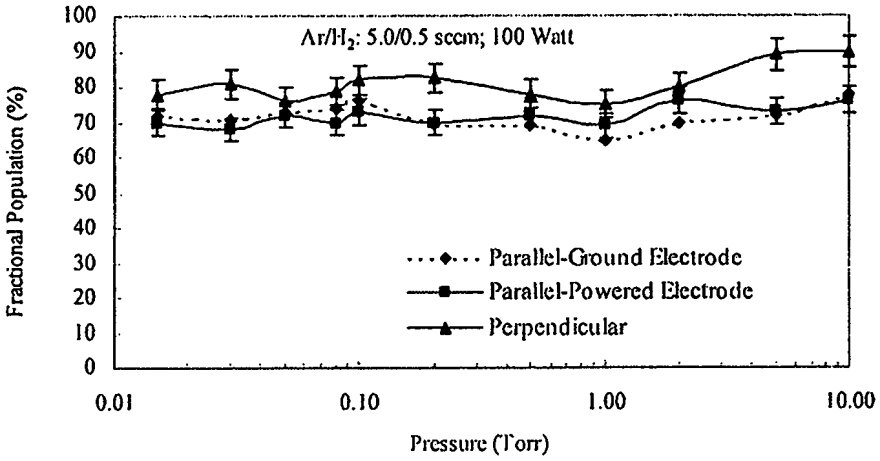

Fig.13. Fractional population of hot hydrogen atoms in n=3 excited state in a capacitively coupled Ar/H_2 discharge at different gas pressures.

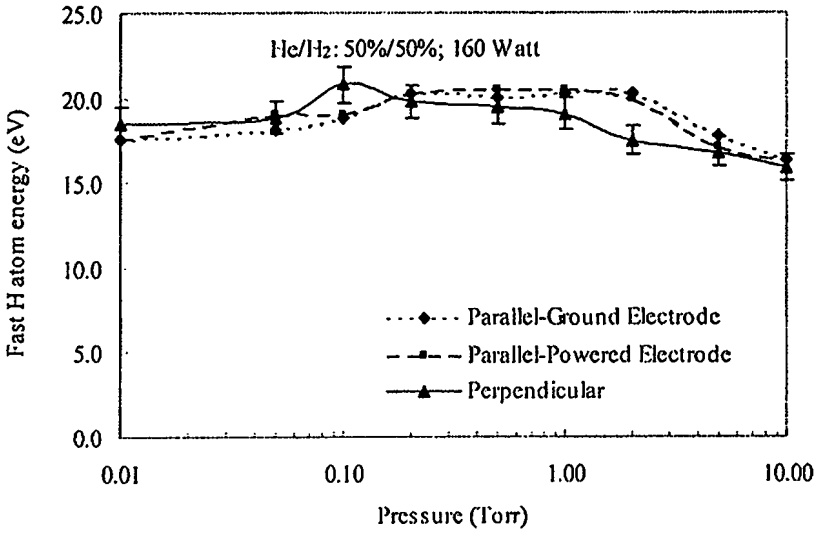

Fig.14. Hot hydrogen atom energy in a capacitively coupled He/H_2 discharge at different gas pressures.

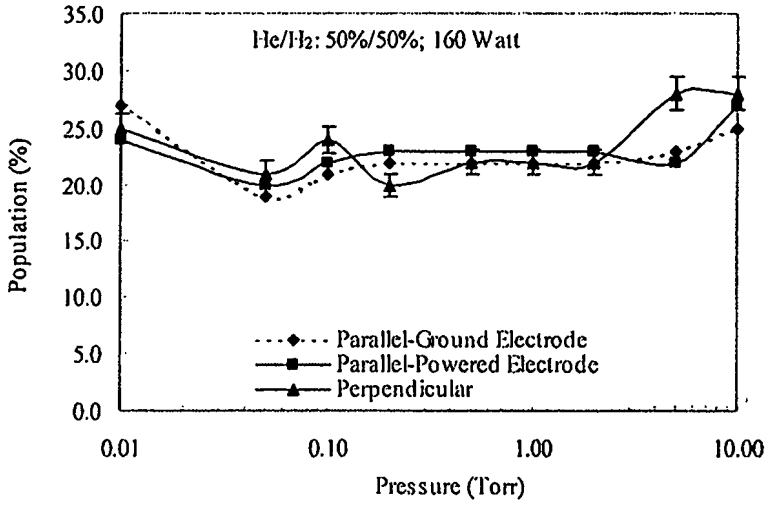

Fig.15. Fractional population of hot hydrogen atoms (n=3 state) in a capacitively coupled He/H_2 discharge at different gas pressures.

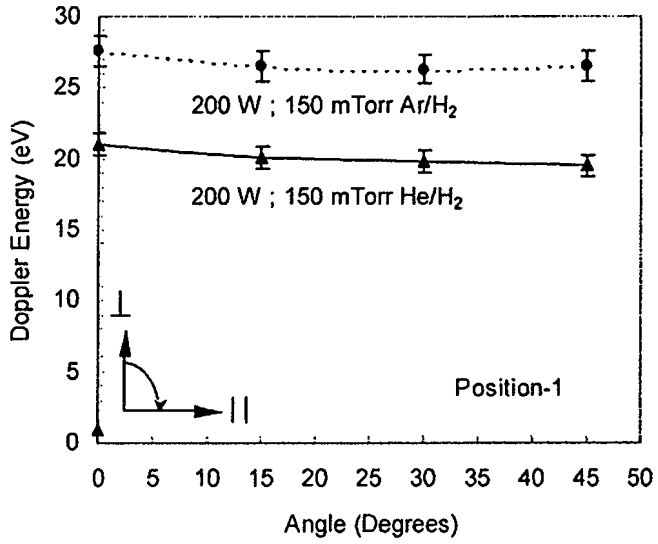

(a)

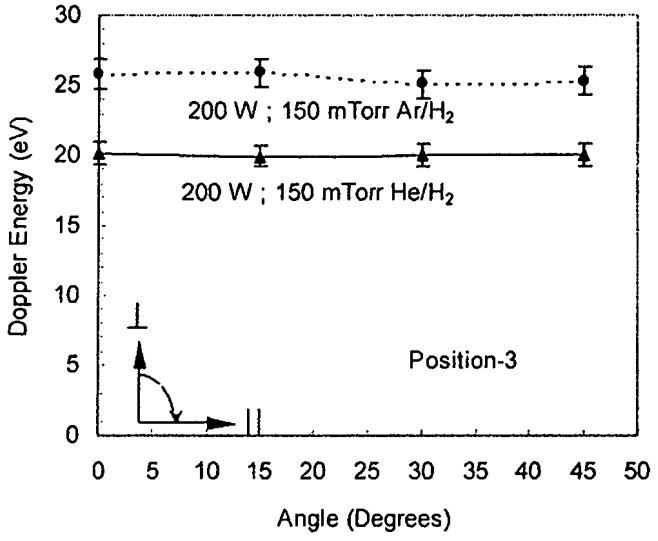

(b)

Fig.16. Angular variation of Doppler energy of hot hydrogen atom in a capacitively coupled radio frequency discharge at 150 mTorr 50%Ar/50%H_2 and 50%He/50%H_2 plasma at 200 W. Plasma emission is sampled at Position 1 (Fig. a) and Position 3 (Fig. b) far away from the region of high field in plasma sheath. Reference is normal to the chamber axis.